Size Control of Silica Nanoparticles and Their Surface Treatment for Fabrication of Dental Nanocomposites

J. W. Kim, L. U. Kim, and C. K. Kim*

School of Chemical Engineering and Materials Science, Chung-Ang University, 221 Huksuk-dong, Dongjak-gu, Seoul, 156-756, Korea

Received June 10, 2006; Revised Manuscript Received November 8, 2006

Nearly monodispersed silica nanoparticles having a controlled size from 5 to 450 nm were synthesized via a sol−gel process, and then the optimum conditions for the surface treatment of the synthesized silica nanoparticles with a silane coupling agent (i.e., 3-methacryloxypropyltrimethoxysilane (γ-MPS)) were explored to produce dental composites exhibiting enhanced adhesion and dispersion of silica nanoparticles in the resin matrix. The particle size was increased by increasing amounts of the catalyst (NH_4OH) and silica precursor (tetraethylorthosilicate, TEOS) and by decreasing the amount of water in the reaction mixtures regardless of solvents used for the synthesis. The particle size prepared by using ethanol as a solvent was significantly larger than that prepared by using methanol as a solvent when the composition of the reaction mixture was fixed. The nanosized particles in the 5−25 nm range were aggregated. The amount of grafted γ-MPS on the surface of the synthesized silica nanoparticles was dependent on the composition of the reaction mixture when an excess amount of γ-MPS was used. When surface treatment was performed at optimum conditions found here, the amount of the grafted γ-MPS per unit surface area of the silica nanoparticles was nearly the same regardless of the particle size. Dispersion of the silica particles in the resin matrix and interfacial adhesion between silica particles and resin matrix were enhanced when surface treated silica nanoparticles were used for preparing dental nanocomposites.

Introduction

Since commercial introduction of polymeric dental restorative composites for restoring anterior teeth in the mid-1960s, their characteristics such as physical properties, manipulative qualities, durability, and wear resistance have improved remarkably.[1,2] As a result, they are widely used instead of amalgam. Composites make up for the weak points of amalgam, such as toxicity from mercury content, corrosion, and low adhesive property.[1−5] In addition, composites have a better aesthetic property than amalgam. The scope of their applications has expanded continuously from small anterior restorations to large posterior restorations and even fixed partial dentures.

Dental composites mainly consist of inorganic fillers and an organic matrix. They are usually classified by the type of silica used as the inorganic filler. There are three types: a direct filling system without filler, a macrofilled system with large particles of glass (macrofiller), and a microfilled system with small particles of silica (microfiller). A direct filling system provides good a color match and is easy to polish, but it undergoes high shrinkage during polymerization and has a high coefficient of thermal expansion. In addition, the softness results in poor surface hardness, a high incidence of fracture under stress, and a high rate of wear. To improve the poor physical properties of a direct filling system, loading dental resins with inorganic filler particles, so-called particulate reinforcement,[6−8] has been introduced. Macrofilled composites that were mainly loaded with large particle size fillers have excellent strength and relatively long-term service, but they have a disadvantage in that the surface smoothness of these restorations is poor. Microfilled composites can reinforce the smoothness of macrofilled composites.[9] Hence, the ideal composite would combine highly filled resins with a small particle size filler. However, unfortunately, it is difficult to load the composites with large amounts of the small size filler since their large surface areas cause significant increases in viscosity. Thus, widespread dental composites usually include not only microfillers but also macrofillers at the same time.[10]

Recently, nanofilled dental composites (or dental nanocomposites) were introduced to the market. Incorporating nanotechnology means a hybrid concept compounding with sub-100 nanoparticles. Dental nanocomposites have been introduced by several manufacturers who claim superior material properties such as excellent optical properties, high mechanical strength, and low abrasion. Furthermore, dental nanocomposites are theoretically purported to have increased wear and fatigue resistance as compared with microfill composites and may favor the achievement of restoratives with better long-term performance. Studies related to the effects of filler size on wear exhibited that a finer particle size for the composite results in less interparticle spacing, more protection of the softer resin matrix, and less filler plucking, all of which lead to enhanced wear resistance for the material.[11−19] These studies were, however, performed on the micrometer sized or microfiller particles rather than nanofillers. The fatigue properties of composite materials may also benefit from the incorporation of small sized particles. The reduced interparticle spacing may result in increased obstacles for dislocation motions and a decreased strain localization.

Previously, it has been suggested that the removal of the materials from the surface of nanocomposites would be less than that from composites filled with micrometer sized particles or prepolymerized resin fillers.[11−19] On the basis of the promising potential of nanocomposites, wear and fatigue resistance of commercial dental nanocomposites were explored previously.[11−19] However, the results indicated that the com-

* To whom correspondence should be addressed. E-mail: ckkim@cau.ac.kr.

10.1021/bm060560b CCC: $37.00
Published on Web 12/14/2006

mercial dental nanocomposites were not likely to provide improved wear and fatigue performance over the traditional microfill composites. Since the commercial dental nanocomposites are mainly nanofilled hybrid composites with some components that are not nanosized (fillers in the nanocomposites are composed of micrometer sized fillers, nanofillers, clusters of nanofillers, or prepolymerized resin filler), the full effects of nanofillers on the wear and fatigue resistance might not be seen. To understand the relationship between nanofiller size, wear, and fatigue resistance, and the mechanical properties of the dental composite, nanocomposites containing uniform sized nanofillers should be prepared. Properties of the nanocomposites also might be dependent on other aspects such as the quality of the interfacial adhesion between the nanofillers and the resin matrix and degree of conversion of the resin matrix. Since the effects expected by the incorporation of the nanoparticles may not be realized without proper surface treatment, silanization of the silica nanoparticles with proper chemicals is also required to provide strong interfacial adhesion.

In this study, nearly monodispersed and spherical silica nanoparticles having different sizes were synthesized via a sol−gel process (i.e., Stöber method),[20] and then the surface of the synthesized silica nanoparticles was treated with 3-methacryloxypropyltrimethoxysilane (γ-MPS) to improve interfacial adhesion between nanofillers and resin matrix. The size of silica nanoparticles was controlled by varying amounts of the reactants and catalyst and by changing the solvent. The optimum condition for the surface treatment of silica nanoparticles with γ-MPS was also explored. The morphology of the dental composites containing silica nanoparticles synthesized here was observed with field emission scanning electron microscopy (FE-SEM). The issues related to the effects of nanofiller size on the wear and fatigue resistance and mechanical strength will be the topic of a forthcoming paper.

Materials and Methods

A sol−gel reaction, the Stöber reaction, was facilitated by hydrolysis and condensation of tetraethylorthosilicate (TEOS, 98+%, Aldrich Chemical Co.) in absolute methanol (MeOH, Aldrich Chemical Co.) or 200-proof ethanol (EtOH, Aldrich Chemical Co.) with a base catalyst. Reagent grade ammonium hydroxide (30% NH_3, Samchun Pure Chemical Co.) was used as the base catalyst. 3-Methacryloxypropyltrimethoxysilane (γ-MPS, 98%, Aldrich Chemical Co.) was used as the silane coupling agent for hydrophobic treatment of the filler. Bis-GMA (99%, Polysciences Inc.) as a base resin, TEGDMA (3G grade, Aldrich Chemical Co.) as a diluent, camphorquinone (CQ, 99%, Aldrich Chemical Co.) as an initiator, and ethyl 4-dimethylaminobenzoate (EDMAB, 99+%, Aldrich Chemical Co.) as an accelerator were used. A radio-opaque barium silicate (H-MAF, Hansol Chemience, Korea, 1 μm primary particle size) was used to prepare hybrid composites.

Silica particles having different sizes were prepared by the Stöber method. The size of silica nanoparticles was controlled by varying amounts of reactants (TEOS and water) and catalyst (ammonium hydroxide) and by changing the solvent (methanol or ethanol). For the synthesis, the solvent, ammonium hydroxide, and deionized water were first mixed, and then TEOS was added. The reaction was performed at 25 °C for 1 h, and then the resulting product was centrifuged at 20 000 rpm for 1 h by using an ultracentrifuge (model:T-1180, Kontron). The obtained silica particles were washed with isopropyl alcohol (IPA) to remove unreacted TEOS. Finally, silica particles were dried in an air circulating oven at 110 °C for 24 h.

The hydrophilic surface of the synthesized nanofiller caused by hydroxyl end groups was treated with γ-MPS to improve interfacial adhesion between resin matrix and nanofiller. The optimum conditions for the surface treatment with γ-MPS were determined by varying the amount of water and catalyst in the methanol solvent. γ-MPS was prehydrolyzed by reacting with deionized distilled water and ammonium hydroxide at 25 °C for 2 h. Silica nanofillers (10 g) were continuously added to the γ-MPS solution and stirred at 1000 rpm for 2 h. On the basis of the knowledge that the maximum amount of silanol existing on the silica particle surface was equal to 8 μmol/m^2,[21] an excess amount of γ-MPS (1 g) was used. After removing unreacted γ-MPS by using an ultracentrifuge, the resulting product was further purified by freeze-drying at −50 °C for 2 days. The surface treated filler was finally cured at 120 °C for 2 h to accomplish the condensation reaction.

The average size of the silica nanoparticles synthesized here was determined by two different methods called P_1 and P_2. The details of each are described next. P_1: Ten transmission electron microscopy (TEM, model: JEM 2000EXII, JEOL, Japan) images were obtained from 10 different specimens for each sample, and then image analysis software (BMI Series v. 4.0) was used to obtain the average particle size and size distribution from TEM images. When particles in the TEM photos did not exhibit a clear boundary or include aggregates, a spherical boundary for each particle was drawn on a monitor, and then the average particle size and size distribution were calculated. P_2: Average particle size and size distribution were also obtained by using a particle size analyzer (model: mastersizer 2000, Malvern).

Existence of the grafted γ-MPS on the surface of the silica nanoparticles was confirmed by solid-state ^{29}Si NMR (400 MHz, model: AVANCE 400WB, DSX-400, Bruker, Germany). In this work, Si−H polarization (CP) was employed for the magnetic-angle spinning (MAS) to obtain high-resolution spectra. The amount of grafted γ-MPS was estimated with elemental analysis (EA, model: EA1110 CE Instrument). According to the Berendsen equation,[22] the amount of grafted γ-MPS is given by eq 1

$$N\ (\mu\text{mol/m}^2) = \frac{10^6 \times P_c}{1200n_c - P_c(M-1)}\frac{1}{S} \qquad (1)$$

where P_c is change in the carbon percentage before and after surface treatment, n_c is the number of carbon atoms in the bonded silane molecule, and M is the molecular weight of the silane molecule. The specific surface area of the silica particles (S, m^2/g) is given by[23]

$$S = 3(\delta R)^{-1} \qquad (2)$$

where δ and R are the mass density of silica particles and their average radius, respectively.

The resin matrix containing 70 wt % of Bis-GMA as a base resin and 30 wt % of TEGDMA as a diluent was used to prepare dental composites. Even though dental composites generally contain more than 70 wt % of inorganic filler, nanocomposites containing silica nanoparticles from 3 to 10 wt % were prepared to compare the dispersion of the nanofillers in the resin matrix. Mixing of the resin matrix and nanofillers was performed in a twin extruder (Bau Tech, model: BA-11, L/D ratio = 40) at 30 °C. The dental composites were placed in a DSC (differential scanning calorimeter, TA Instruments, TA-2100) sample pan (6 mm diameter × 2 mm thickness) and polymerized by irradiating with visible light from a light source (λ_{max} 460 nm, intensity 600 mW/cm^2, VIP Junior Curing Light, BISCO Inc.) under nitrogen-purged conditions. To investigate changes in the dispersion of the silica nanofiller, cured dental composites were fractured in liquid nitrogen conditions, and then the morphology of the fracture surface was observed with FE-SEM (field emission scanning electron microscopy, JSM-6700F, JEOL).

Results and Discussion

Changes in the Size of Silica Nanoparticles. Nearly monodispersed and spherical silica particles were synthesized by a sol−gel process (i.e., the Stöber method). The average size

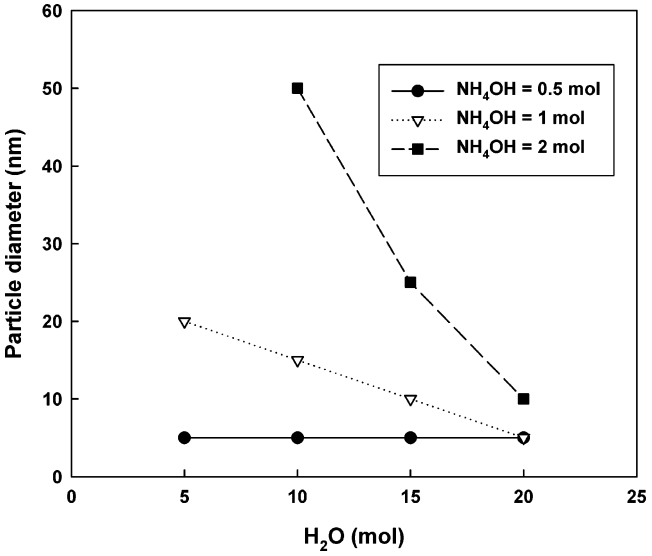

Figure 1. Changes in the silica particle size as a function of water concentration. Note that the amount of methanol (1 L) and TEOS concentration (0.28 mol) were fixed for synthesis.

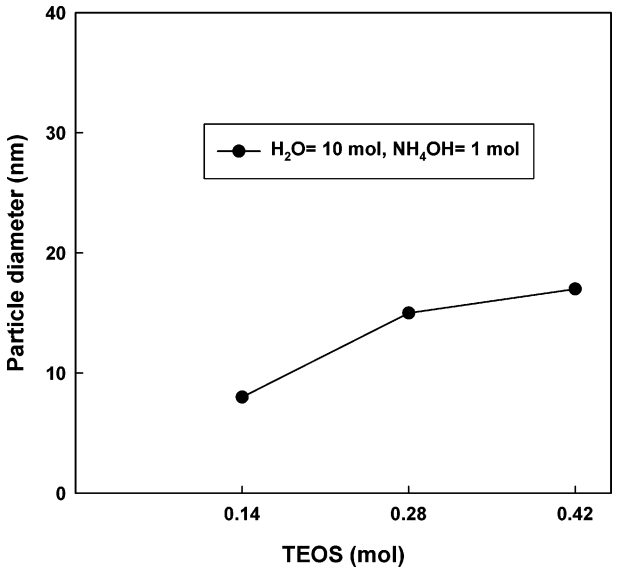

Figure 2. Changes in the silica particles size as a function of TEOS concentration. Note that the amount of methanol (1 L), water concentration (10 mol), and NH_4OH concentration (1 mol) were fixed for synthesis.

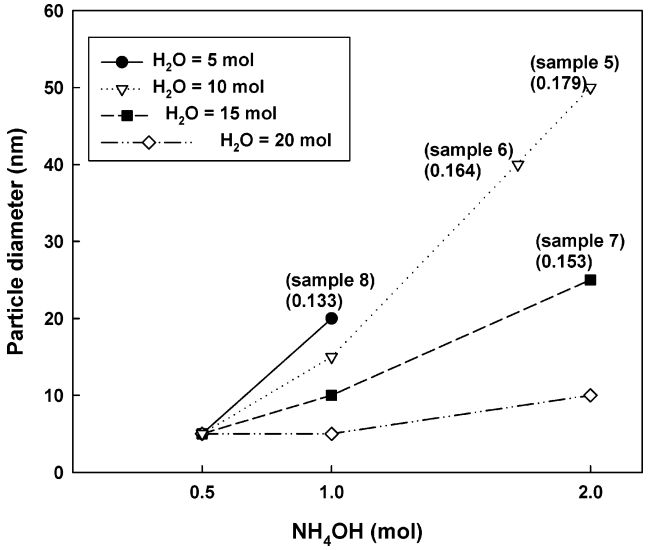

Figure 3. Changes in the silica particle size as a function of NH_4OH concentration. Note that the amount of methanol (1 L) and TEOS concentration (0.28 mol) were fixed for synthesis. Note that the number in the parenthesis indicates the uniformity of particles (i.e., the absolute deviation from the median).

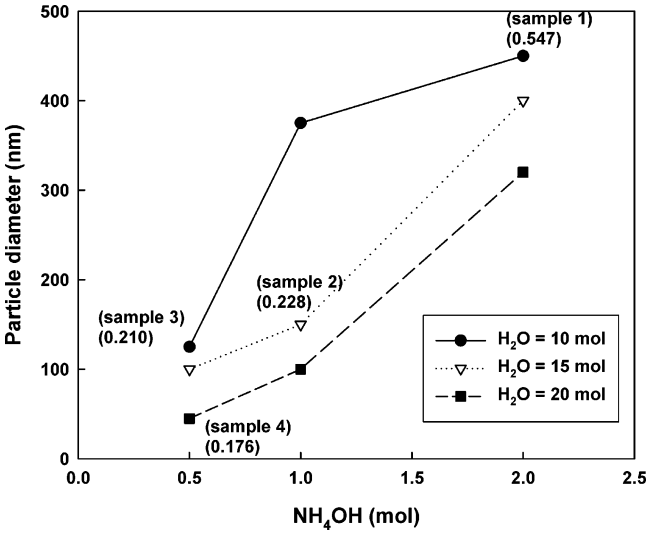

Figure 4. Changes in the silica particle size as a function of NH_4OH concentration. Note that the amount of ethanol (1 L) and TEOS concentration (0.28 mol) were fixed for synthesis. Note that the number in parentheses indicates the uniformity of particles (i.e., the absolute deviation from the median).

of the silica nanoparticles synthesized here was determined by two different methods called P_1 and P_2. The results measured with both methods were nearly the same when the average particle size was greater than about 100 nm. However, when the particle size was below about 100 nm, the average particle size measured with light scattering (P_2) was always greater than that calculated from TEM images (P_1) for the same sample. It might stem from poor dispersion of nanoparticles in the medium or aggregates formed with primary nanoparticles. Because of these, the results obtained from P_1 might be more reliable than those obtained from P_2. The average particle size reported here was that calculated from TEM images using image analysis software.

In the Stöber method, the size of the silica particles was dependent on the kind of solvent and the amount of reactants (water and TEOS) and catalyst (ammonium hydroxide). Note that the results presented in Figures 1−3 were obtained with the methanol solvent, while those presented in Figures 4 and 5 were obtained with the ethanol solvent. Figure 1 exhibited changes in the particle size with water concentrations when the concentrations of TEOS and NH_4OH were fixed. The decline of particle size was observed by increasing the water concentration. However, when the NH_4OH concentration was equal to or less than 0.5 mol, the particle size (5 nm) was not further reduced regardless of the water concentration. The particle size was increased by increasing the TEOS concentration in the reaction mixture when the concentrations of water and NH_4OH were fixed as shown in Figure 2. An increase in the particle size was also observed by increasing the NH_4OH concentration when the concentrations of water and TEOS were fixed (Figure 3). Consequently, the incline in the particle size was observed by increasing the TEOS and NH_4OH concentration and by decreasing the water concentration. Silica nanoparticles having various sizes from 5 to 50 nm could be synthesized by

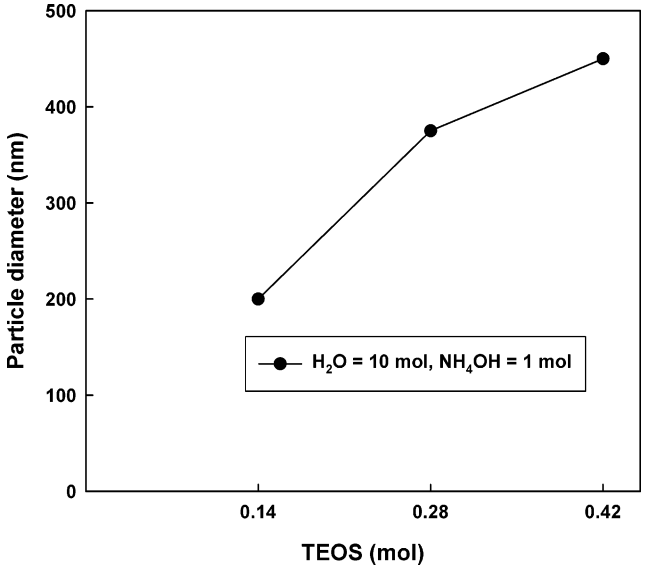

Figure 5. Changes in the silica particle size as a function of TEOS concentration. Note that amount of ethanol (1 L), water concentration (10 mol), and NH_4OH concentration (1 mol) were fixed for synthesis.

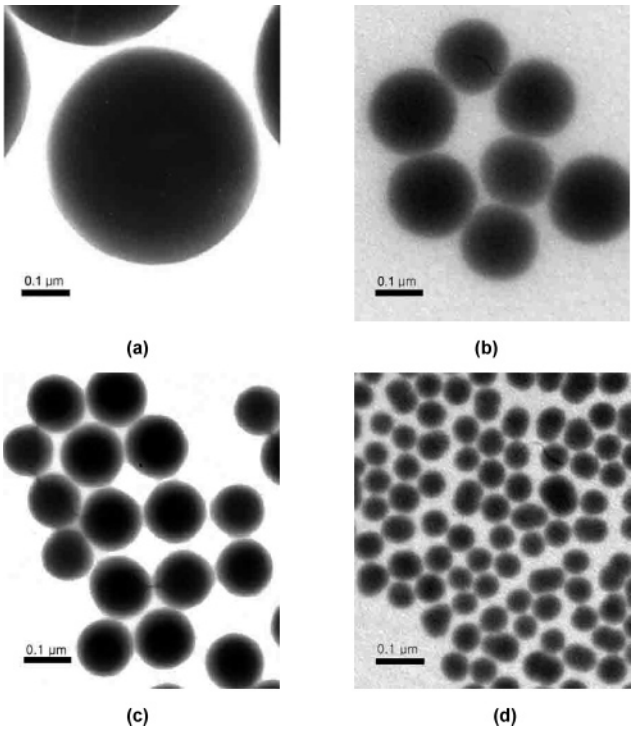

Figure 6. TEM microphotographs of the nearly monodispersed silica particles synthesized by using ethanol as a solvent. (a) Sample 1 in Figure 4 (average diameter: 450 nm), (b) sample 2 in Figure 4 (average diameter: 150 nm), (c) sample 3 in Figure 4 (average diameter: 125 nm), and (d) sample 4 in Figure 4 (average diameter: 50 nm).

controlling the concentration of reactants and catalyst and by using methanol as a solvent.

To produce silica particles larger than 50 nm, ethanol was used instead of methanol as a solvent. As shown in Figures 4 and 5, the results examined with ethanol exhibited the same tendency with those examined with methanol; the decline in the particle size was also observed by increasing the water concentration and decreasing the concentrations of TEOS and NH_4OH. However, the size of particles synthesized with the ethanol solvent was significantly larger than that synthesized with the methanol solvent. It was known that changes in the

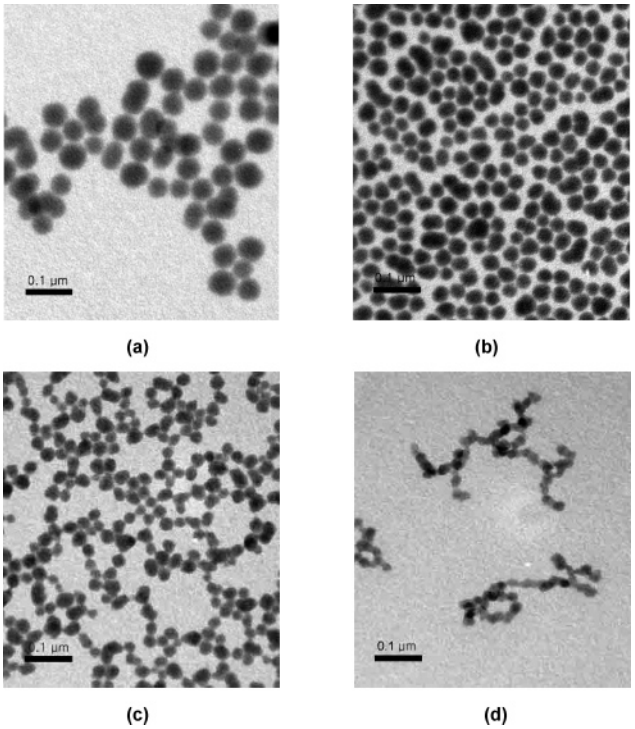

Figure 7. TEM microphotographs of the silica nanoparticles synthesized by using methanol as a solvent. (a) Sample 5 in Figure 3 (average diameter: 50 nm), (b) sample 6 in Figure 3 (average diameter: 40 nm), (c) sample 7 in Figure 3 (average diameter: 25 nm), and (d) sample 8 in Figure 3 (average diameter: 20 nm).

particle size with the solvent used for the synthesis of silica particles stemmed from the differences in the size of nuclei formed in each solvent.[24] The nuclei created in the methanol solvent are smaller than those created in the ethanol solvent because the supersaturation ratio of the hydrolyzed monomer in the methanol solvent is higher than that in the ethanol solvent.[24] Note that silica particles were not formed when the concentration of water and catalyst was lower than 10 and 0.5 mol, respectively. The particle size was not further reduced from 45 nm, even though the water concentration was increased over 20 mol. Accordingly, the size of the silica particles was not reduced under 45 nm when ethanol was used as a solvent. In summary, silica nanoparticles having various sizes with a range from 5 to 450 nm could be produced by controlling the concentrations of reactant and catalyst and by changing the solvent.

Figures 6 exhibited TEM microphotographs of silica nanoparticles produced by using ethanol as a solvent. When ethanol was used as a solvent, nearly monodispersed and spherical silica particles were formed. The morphology of particles synthesized by using methanol as a solvent was dependent on the particle size as exhibited in Figure 7. Nearly monodispersed and spherical nanoparticles were formed when the particle size was larger than 25 nm. However, aggregates of silica nanoparticles having a network structure began to form when their size was below about 25 nm. These results might stem from the following reasons. The smaller the particles that formed, the more particles produced. Since small particles have a higher surface tension than large particles, they easily aggregate to make their surface more stable. Because of these, silica particles below about 25 nm formed a network structure caused by aggregation, while spherical particles were formed without aggregation when their size was greater than 25 nm.

Surface Modification of Silica Particles with γ-MPS. Silica particles produced here might have hydrophilic properties

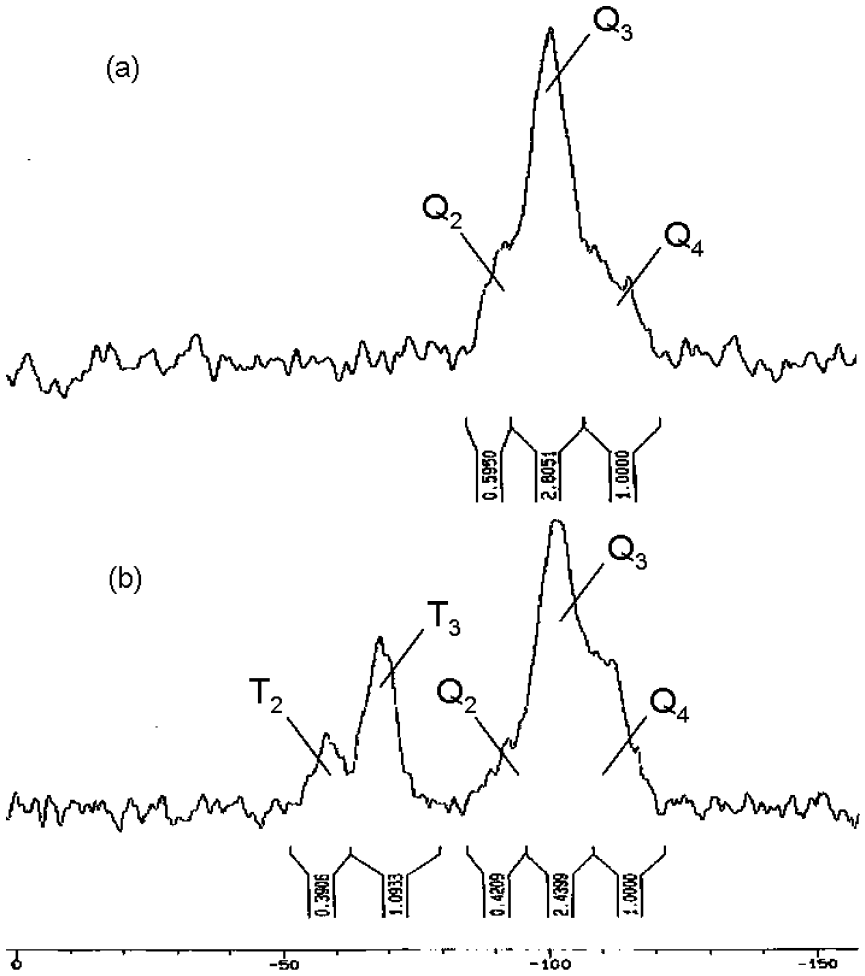

Figure 8. Solid-state ^{29}Si NMR spectra of the silica particles (average diameter: 45 nm) synthesized in this study. (a) Before surface treatment and (b) after γ-MPS surface treatment.

because of hydroxyl groups existing on the particle surface. Since mechanical properties of a dental composite mainly depend on the interfacial adhesion between inorganic fillers and organic matrix, improvement of the interfacial adhesion might be one of the important issues in producing a successful dental composite. The hydrophilic surface of the synthesized silica particles was treated with γ-MPS to improve interfacial adhesion between resin matrix and silica particles. The more grafted γ-MPS that existed on the particle surface, the better the interfacial adhesion expected. On the basis of this hypothesis, the amount of grafted γ-MPS was characterized as a function of water and catalyst (NH_4OH) concentration to find optimum reaction conditions. Note that a fixed amount of γ-MPS and solvent (methanol) was used in here. Characteristics of the grafted γ-MPS and amount of grafted γ-MPS were examined with ^{29}Si− NMR and elemental analysis, respectively.

Figure 8 exhibited ^{29}Si− NMR spectrum of silica nanoparticles (45 nm) synthesized here (Figure 8a) and that of silica nanoparticles treated with γ-MPS. The ^{29}Si− NMR spectrum of untreated particles exhibited only three peaks in the Q region. The peaks (i.e., designated in Figure 8a as Q_4 (−104 to approximately −120 ppm), Q_3 (−94 to approximately −104 ppm), and Q_2 (−85 to approximately −94 ppm)) correspond to $Si(OSi)_4$, $Si(OSi)_3(OH)$, and $Si(OSi)_2(OH)_2$, respectively−.[25,26] It means that the amount of ethoxy groups comes from TEOS (i.e., carbon content in the untreated particles is negligible). When particles were treated with γ-MPS, two peaks in the T region, which were not observed with untreated particles, were observed (Figure 8b). The peaks designated as T_3 (−65 to approximately −66 ppm) and T_2 (−55 to approximately −56 ppm) correspond to $Si(OSi)_3(CH_3)$ and $Si(OSi)_2(OH)(CH_3)$, respectively.[25−,26] These results indicated that hydrocarbons stemmed from the grafted γ-MPS existed on the surface of the treated silica particles. In comparing the relative ratio of the Q_4

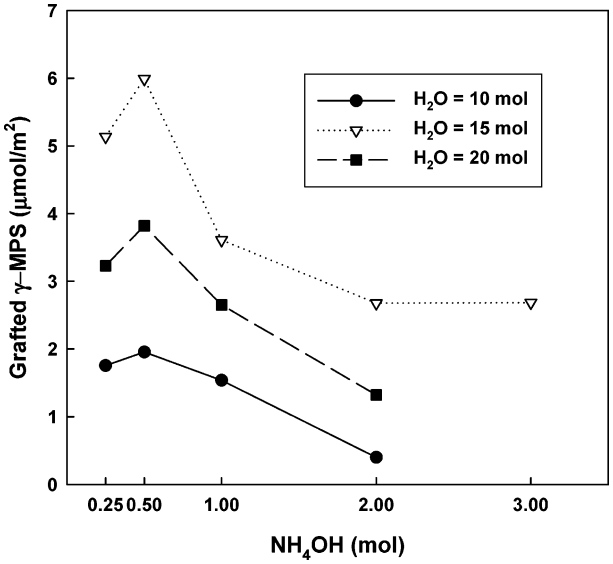

Figure 9. Changes in the amount of grafted γ-MPS with NH_4OH concentration. Each experiment was performed with 10 g of silica particles. Note that the γ-MPS concentration (1 g) and amount of methanol solvent (0.2 L) were fixed.

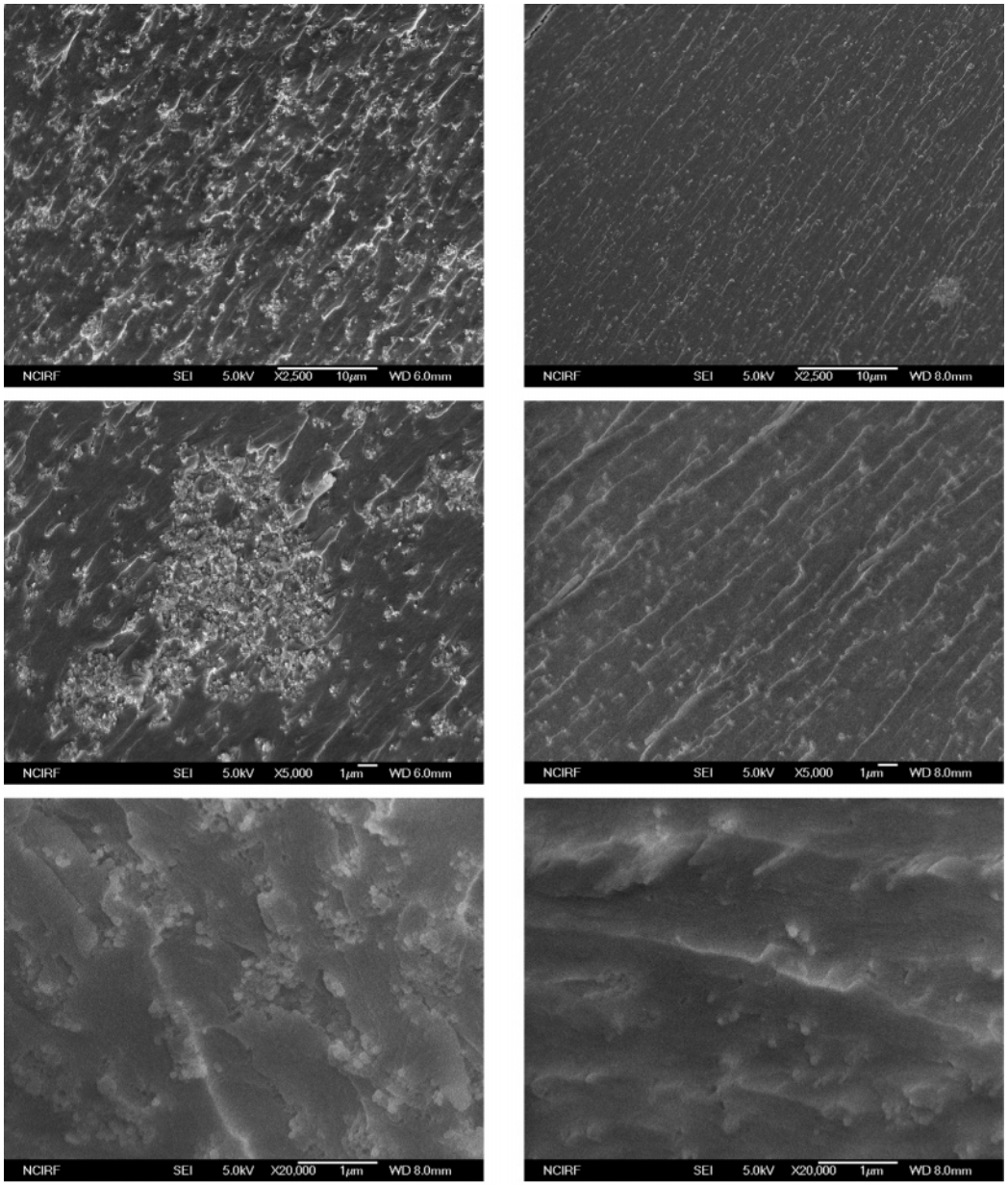

Figure 10. FE-SEM microphotographs exhibiting the changes in dispersion and adhesion of silica nanoparticles (45 nm, 10 wt %) embedded in the organic resin matrix. Note that each sample was observed at three different magnifications (2500×, 5000×, and 20 000×). (a) Composites prepared by using untreated silica nanoparticles and (b) composites prepared by using surface treated silica nanoparticles.

area to the total area corresponding to the Q region of the surface treated particles with that of the untreated particles, the former was larger than the latter. This also means that Si bonded with hydroxyl groups (Q_2 and Q_3 peaks) (i.e., $Si(OSi)_3(OH)$ and $Si(OSi)_2(OH)_2$) was changed to $Si(OSi)_4$ (Q_4 peak) caused by the reaction between hydroxyl groups and γ-MPS.

The amount of grafted γ-MPS (μmol/m^2) on the particles surface was calculated from the carbon content measured with elemental analysis by using eq 1. Comparing the amount of carbon content of the treated particles with that of the untreated particles, the former was always greater than that of the latter. Note that the carbon content in the untreated particles was negligible. These results also indicated that γ-MPS was reacted with the hydroxyl groups on the silica particle surface. Figure 9 exhibited changes in the amount of grafted γ-MPS on the silica particle surface (average particle diameter: 45 nm) with the NH_4OH content when the amount of water was fixed. The amount of grafted γ-MPS first increased with increasing NH_4OH content, went through a maximum, and then decreased. A similar trend was observed at other water contents. The amount of grafted γ-MPS was affected by not only the amount of water but also that of NH_4OH. Homocondensation between γ-MPS monomers also occurred concomitantly with the reaction between hydroxyl groups in the silica particles and γ-MPS.[27] Since these are competing reactions, the amount of grafted γ-MPS might be dependent on the reaction conditions. Note that the resulting product stemming from the homocondensation reaction was readily separated from the silica particles by centrifuging. Within the experimental conditions examined here, the silica particles covered with a maximum amount of γ-MPS (6.0 μmol/m^2, see Figure 9) was prepared when the reaction mixture contained 15 mol of water and 0.5 mol of NH_4OH.

To investigate the particle size effects on the amount of the grafted γ-MPS, surface treatment was performed with silica particles having different sizes (i.e., 15, 100, and 150 nm) at optimum conditions determined. The amount of grafted γ-MPS per unit area was nearly the same regardless of particle size (6.0 μmol/m^2 $\pm$ 0.08). These results indicated that the amount

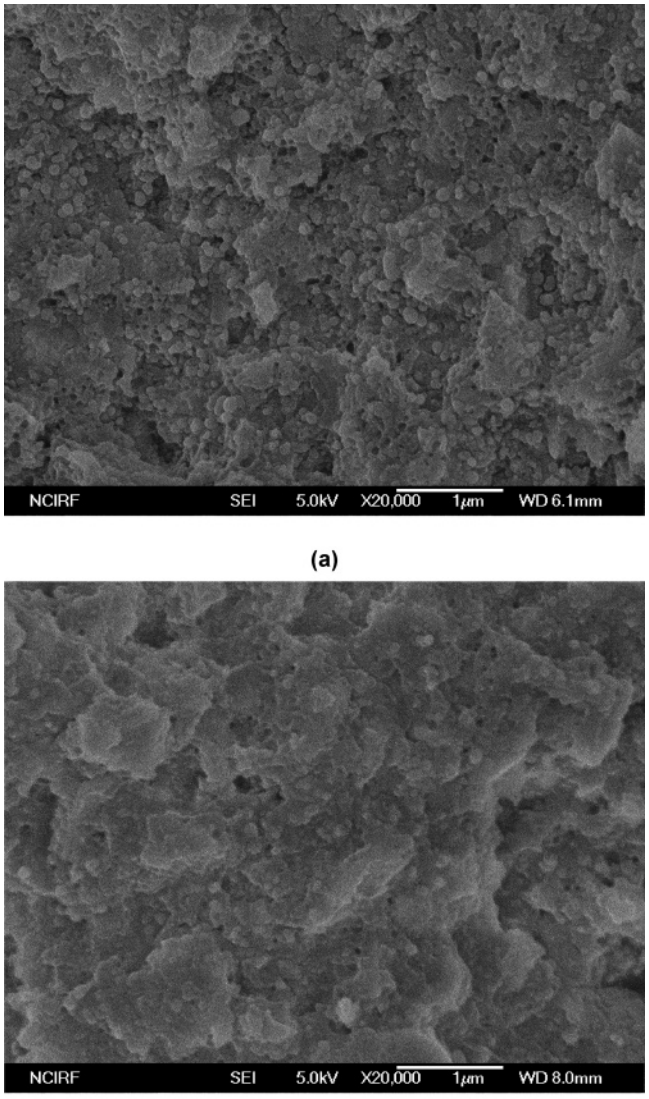

Figure 11. FE-SEM microphotographs of dental composites. Each composite contains 65 wt % of barium silicate (primary particle size, 1 μm) and 10 wt % of silica nanoparticles (primary particle size, 45 nm). (a) Dental composite containing untreated silica nanoparticles and (b) dental composite containing surface treated silica nanoparticles.

of grafted γ-MPS per unit area was independent of the particles size when reaction conditions were fixed.

Dispersion of Silica Particles in the Composites. To explore the effects of surface treatment with γ-MPS on the particle dispersion in the resin matrix, composites containing surface treated silica nanoparticles (45 nm) or untreated silica nanoparticles were prepared. The resin matrix used here in this study consisted of 70 wt % Bis-GMA as a base resin and 30 wt % TEGDMA as a diluent. Figure 10 exhibited cross-sectional morphologies of dental composites containing 10 wt % surface treated (or untreated) silica nanoparticles observed with FE-SEM at various magnifications. Dispersion of treated particles in the resin matrix was much better than that of untreated particles. Composites prepared from the untreated particles contained particle aggregates, while those prepared from the treated particles did not contain particle aggregates. Furthermore, surface treated silica particles exhibited better adhesion with the resin matrix than untreated silica particles. It was true that other composites contained less than 10 wt % silica nanoparticles. Enhanced dispersion in the resin matrix and interfacial adhesion with the resin matrix of the treated silica particles might come from the chemical bonding between methacrylate groups in γ-MPS and that in the resin matrix as well as hydrophobic interactions between resin matrix and grafted γ-MPS. Figure 11 exhibited cross-sectional morphologies of hybrid dental composites containing 65 wt % a radio-opaque barium silicate (1 μm primary particle size) and 10 wt % silica nanoparticles prepared here (45 nm). The surface treated particles were better adhered to the polymer matrix because fewer were visible after surface treatment (more are invisible because they are covered by the matrix). There are also fewer black holes in the matrix, an indication of pullout of poorly attached particles. Thus, dispersion of the silica particles in the resin matrix and interfacial adhesion between silica particles and resin matrix were enhanced by using γ-MPS grafted silica nanoparticles.

Conclusion

Nearly monodispersed and spherical silica nanoparticles having various sizes from 5 to 450 nm were synthesized via a sol−gel process. The particle size was increased by decreasing the water concentration and by increasing the TEOS and NH_4-OH concentrations regardless of solvent used for the synthesis. Silica particles having an average size from 5 to 50 nm were formed when methanol was used as a solvent, while those having an average size from 45 to 450 nm were formed when ethanol was used as a solvent. The nanosized particles in the 5−25 nm range were aggregated. The hydrophilic surface of the prepared silica particles caused by hydroxyl groups existing on the particle surface was treated with γ-MPS to improve dispersion of particles in the resin matrix and interfacial adhesion between resin matrix and particles. Reaction characteristics between particles and γ-MPS were analyzed with ^{29}Si− NMR. The amount of grafted γ-MPS per unit area characterized with elemental analysis was changed from 0.4 to 6.0 μmol/m^2 with reaction conditions. When surface treatment was performed at optimum reaction conditions, the amount of grafted γ-MPS per unit area was nearly the same (6.0 ± 0.08 μmol/m^2) regardless of particle size. Dental nanocomposites containing surface treated silica nanoparticles exhibited better dispersion of the particles in the resin matrix and interfacial adhesion than those containing untreated silica nanoparticles.

Acknowledgment. This study was supported by a grant of the Korea Health 21 R&D Project, Ministry of Health and Welfare, Republic of Korea (03-PJ1-Ch09-0001).

References and Notes

(1) Donald, M.; Orson, D. W. *J. Am. Dent. Assoc., JADA* **1976**, *92*, 1189.
(2) Leonard, P.; Ellse, M. C. *J. Am. Dent. Assoc., JADA* **1976**, *92*, 1195.
(3) Schoonover, I. C.; Sounder, W. *J. Am. Dent. Assoc., JADA* **1941**, *28*, 1278.
(4) Pashley, E. L.; Comer, R. W.; Parry, E. E.; Pashley, D. H. *Oper. Dent.* **1991**, *16*, 82.
(5) Staninec, M.; Holt, M. *J. Prosthet. Dent.* **1988**, *59*, 397.
(6) Luts, F.; Phillips, R. W. *J. Prosthet. Dent.* **1983**, *50*, 480.
(7) Hosoda, H.; Yamata, T.; Inokoshi, S. *J. Prosthet. Dent.* **1990**, *64*, 669.
(8) Willems, G.; Lambrechts, P.; Braem, M.; Celis, J. P.; Vanherle, G. *Dent. Mater.* **1992**, *8*, 310.
(9) Bayne, S. C.; Heymann, H. O.; Swift, E. J. *J. Am. Dent. Assoc.* **1994**, *125*, 687.
(10) kim, K. H.; Ong, J. L.; Okuno, O. *J. Prosthet. Dent.* **2002**, ***87***, 642.
(11) Cui, D.; Gao, H. *Biotechnol. Prog.* **2003**, *19*, 683.
(12) Suzuki, S.; Leinfelder, K. L.; Kaway, K.; Tsuchtani, Y. *Am. J. Dent.* **1995**, *8*, 173.

(13) Venhoven, B. A. M.; de Gee, A. J.; Werner, A.; Davidso, C. L. *Biomaterials* **1996**, *17*, 735.
(14) Jørgensen, K. D.; Asmussen, E. *Quintessence Int*. **1978**, *9*, 73.
(15) Bayne, S. C.; Taylor, D. F.; Heymann, H. O. *Dent Mater*. **1992**, *8*, 305.
(16) Xing, X. S.; Li, R. K. Y. *Wear* **2004**, *256*, 21.
(17) Sawyer, W. G.; Freudenberg, D.; Bhimaraj, M.; Schadler, L. *Wear* **2003**, *254*, 573.
(18) Mitra, S. B.; Wu, D.; Holmes, B. N. *J. Am. Dent. Assoc.* **2003**, *134*, 1382.
(19) Shi, G.; Zhang, M. Q.; Rong, M. Z.; Wetzel, B.; Friedrich, K. *Wear* **2003**, *254*, 784.
(20) Stöber, W.; Fink, A.; Bohn, E. *J. Colloid Interface Sci.* **1968**, *26*, 62.
(21) Bourgeat-Lami, E.; Lang, J. *J. Colloid Interface Sci*. **1998**, *197*, 293.
(22) Berendsen, G. E.; De Gala, L. *J. Liq. Chromatogr*. **1978**, *1*, 561.
(23) Philipse, A. P.; Vrij, A. *J. Colloid Interface Sci*. **1989**, *128*, 121.
(24) Green, D. L.; Lin, J. S.; Hu, M. Z.-C.; Schaefer, D. W.; Harris, M. T. *J. Colloid Interface Sci.* **2003**, *266*, 346.
(25) Glaser, R. H.; Wilkes, G. L. *J. Non-Cryst. Solids* **1989**, *113*, 73.
(26) Lippmaa, E.; Mägi, M.; Samoson, A.; Engelhardt, G.; Grmmer, A. R. *J. Am. Chem. Soc*. **1980**, *102*, 4889.
(27) Posthumus, W.; Magusin, P. C. M. M.; Brokken-Zijp, J. C. M.; Tinnemans, A .H. A.; van der Linde, R. *J. Colloid Interface Sci.* **2004**, *269*, 109.

BM060560B